Behavioral/Cognitive

Excitatory Contribution to Binocular Interactions in Human Visual Cortex Is Reduced in Strabismic Amblyopia

Chuan Hou (侯川), Terence L. Tyson, Ismet J. Uner, Spero C. Nicholas, and Preeti Verghese
Smith-Kettlewell Eye Research Institute, San Francisco, California 94115

Binocular summation in strabismic amblyopia is typically reported as being absent or greatly reduced in behavioral studies and is thought to be because of a preferential loss of excitatory interactions between the eyes. Here, we studied how excitatory and suppressive interactions contribute to binocular contrast interactions along the visual cortical hierarchy of humans with strabismic and anisometropic amblyopia in both sexes, using source-imaged steady-state visual evoked potentials (SSVEP) over a wide range of relative contrast between the two eyes. Dichoptic parallel grating stimuli modulated at unique temporal frequencies in each eye allowed us to quantify spectral response components associated with monocular inputs (self-terms) and the response components because of interaction of the inputs of the two eyes [intermodulation (IM) terms]. Although anisometropic amblyopes revealed a similar pattern of responses to normal-vision observers, strabismic amblyopes exhibited substantially reduced IM responses across cortical regions of interest (V1, V3a, hV4, hMT+ and lateral occipital cortex), indicating reduced interocular interactions in visual cortex. A contrast gain control model that simultaneously fits self- and IM-term responses within each cortical area revealed different patterns of binocular interactions between individuals with normal and disrupted binocularity. Our model fits show that in strabismic amblyopia, the excitatory contribution to binocular interactions is significantly reduced in both V1 and extra-striate cortex, whereas suppressive contributions remain intact. Our results provide robust electrophysiological evidence supporting the view that disruption of binocular interactions in strabismus or amblyopia is because of preferential loss of excitatory interactions between the eyes.

Key words: **amblyopia; binocular interactions; excitatory interactions; source-imaged SSVEP; suppressive interactions; visual cortex**

Significance Statement

We studied how excitatory and suppressive interactions contribute to binocular contrast interactions along the visual cortical hierarchy of humans with normal and amblyopic vision, using source-imaged SSVEP and frequency-domain analysis of dichoptic stimuli over a wide range of relative contrast between the two eyes. A dichoptic contrast gain control model was used to characterize these interactions in amblyopia and provided a quantitative comparison to normal vision. Our model fits revealed different patterns of binocular interactions between normal and amblyopic vision. Strabismic amblyopia significantly reduced excitatory contributions to binocular interactions, whereas suppressive contributions remained intact. Our results provide robust evidence supporting the view that the preferential loss of excitatory interactions disrupts binocular interactions in strabismic amblyopia.

Introduction

Amblyopia is a developmental disorder of spatial vision, characterized by visual acuity loss and abnormal binocularity (Holmes and Clarke, 2006). Strabismus (misaligned eyes) and anisometropia (unequal refractive error between the two eyes) are the most common causes of amblyopia (Woodruff et al., 1994; Simons, 2005). Behavioral studies report that binocular summation, the superiority of binocular vision over monocular vision (Campbell and Green, 1965), is absent or greatly reduced in strabismic amblyopia (Lema and Blake, 1977; Levi et al., 1980; Pardhan and Gilchrist, 1992; Dorr et al., 2019). The loss of binocular neurons in the visual cortex is assumed to underlie the defects of binocular summation and stereopsis in strabismic animals (Hubel and Wiesel, 1965; Harwerth et al., 1984) and humans (Lema and Blake, 1977; Levi et al., 1979). It has been proposed that the neuroanatomical basis for the defects of binocular summation in strabismic animals is because of the preferential loss of excitatory intrinsic connections between neighboring ocular dominance columns (Lowel and Singer, 1992), leaving only inhibitory projections in the majority of neurons (Sengpiel and Blakemore,

Received Feb. 3, 2021; revised Aug. 12, 2021; accepted Aug. 13, 2021.

Author contributions: C.H. designed research; C.H., T.L.T., and I.J.U. performed research; S.C.N. contributed unpublished reagents/analytic tools; C.H., S.C.N., and P.V. analyzed data; C.H. and P.V. wrote the paper.

This work was supported by National Institutes of Health Grant R01-EY025018 to C.H. We thank Dr. Jeffrey J. Tsai for sharing and providing the model script used in Tsai et al. (2012) and Margaret Q. McGovern for assistance in recruiting the participants.

The authors declare no competing financial interests.

Correspondence should be addressed to Chuan Hou at chuanhou@ski.org.

https://doi.org/10.1523/JNEUROSCI.0268-21.2021

1996). This is consistent with behavioral studies that reported an absence of binocular summation (Levi et al., 1979) but with normal dichoptic masking in human strabismus and/or amblyopia (Huang et al., 2011; Levi et al., 1979). An MEG source-imaging study (Chadnova et al., 2017) also reported an equal dichoptic masking effect in V1 between the two eyes in human strabismic amblyopia, supporting intact suppressive interactions in amblyopia between the two eyes.

However, there is an ongoing debate about the lack of binocular summation in strabismic amblyopia in a number of psychophysical studies (Baker et al., 2007, 2008; Mansouri et al., 2008). Baker et al. (2007) showed intact binocular summation in human strabismic amblyopia after they increased stimulus contrast to the amblyopic eye, indicating that strabismic amblyopia has latent binocular function that is normally hidden because of suppressive interactions from the fellow eye under normal viewing conditions (equal contrast in the two eyes). Importantly, Baker et al. (2007) suggest an alternative explanation for the absence of binocular summation in strabismus and/or amblyopia reported in earlier studies when equal contrast was presented to the two eyes (Lema and Blake, 1977; Levi et al., 1980; Pardhan and Gilchrist, 1992; Dorr et al., 2019). Baker et al. (2007) specifically suggest that boosting the signal to the amblyopic eye (by increasing the contrast in the amblyopic eye) can lead to normal levels of binocular summation (Hess et al., 2014).

Therefore, in this study, we set out to answer the following questions: (1) whether there are latent binocular interactions in visual cortex in human strabismus and/or amblyopia and (2) how excitatory and suppressive interactions contribute to binocular contrast interactions along the visual cortical hierarchy in human strabismus and/or amblyopia. To address these questions, we used source-imaged steady-state visual evoked potentials (SSVEP) and frequency-domain analysis of dichoptic stimuli over a wide range of relative contrasts between the two eyes. This allowed us to quantify spectral response components associated with monocular inputs (self-terms) and the response components because of interaction of the inputs of the two eyes [intermodulation (IM) terms]. Self-term responses reveal the responses to the input of each eye, and IM-term responses are a direct measure of interocular interactions in visual cortex (Brown et al., 1999). We used a contrast gain control model (Tsai et al., 2012) to study how excitatory and suppressive interactions contribute to binocular contrast interaction along the visual cortical hierarchy in humans with normal and disrupted binocular vision.

Materials and Methods

Participants. A total of 42 adults between 21 and 68 years old (mean ± SD, 42.69 ± 14.33) of both sexes (17 males) participated in this study. Twenty-seven participants with unilateral amblyopia had visual acuity (VA) equal or worse than 20/25 [0.1 logarithm of the minimum angle of resolution (logMAR)] in the amblyopic eye, and VA equal or better than 20/20 (0 logMAR) in the fellow eye, measured with a Bailey–Lovie LogMAR chart at 6 m distance with the best optical correction. The study included 15 individuals with 20/20 or better VA in each eye (Controls), who also participated in a previous study of normal binocular interactions (Hou et al., 2020). There was no significant difference (p = 0.7855) in age between Controls (mean ± SD, 43.53 ± 15.19) and amblyopic participants (mean ± SD, 42.2 ± 14.11). All participants were recruited from the San Francisco Bay Area with a research advertisement and were refracted under noncycloplegic conditions by C. H., a pediatric ophthalmologist, before the experiments. Amblyopic participants were classified into the following subgroups. Anisometropic amblyopia (hereafter referred to as Aniso; n = 10) was defined as unequal refractive error between the two eyes of at least 1 diopter in any meridian and with no constant ocular deviation or history of strabismus surgery. Strabismic amblyopia (hereafter referred to as Strab; n = 17) was defined as a constant ocular deviation or a history of prior strabismus surgery with or without anisometropia. There was no significant difference (p = 0.8799) in logMAR VA in the amblyopic eye between the Aniso (mean ± SD, 0.46 ± 0.17) and the Strab (mean ± SD, 0.47 ± 0.19) groups. Depending on whether fusion was present with nonius alignment under a mirror stereoscope or an amblyoscope, Strabs were classified into Strab-with-fusion (n = 10) and Strab-without-fusion (n = 7) subgroups. Clinical details of the amblyopic participants are provided in Table 1. Stereoacuity was measured with random dot Stereo Butterfly card (Stereo Optical) at near distance (40 cm) with the best optical correction. Controls had stereoacuity of at least 40 arcsec. Anisos had measurable stereoacuity, whereas most Strabs had nonmeasurable stereoacuity, as seen in Table 1. The dominant and nondominant eye in Controls was determined using the hole-in-the card test. Participants who had congenital cataract, eccentric fixation (measured by a direct ophthalmoscope), and nystagmus or latent nystagmus (nystagmus that appears when covering one eye) were excluded from the study. The research protocol conformed to the tenets of the Declaration of Helsinki and was approved by the Institutional Review Board of the Smith-Kettlewell Eye Research Institute. Written informed consent was obtained before the experiments.

Stimuli. Figure 1 illustrates the stimuli and experimental design. A pair of parallel sinusoidal gratings of spatial frequency 2 cycle/degree was presented on two matched Sony Trinitron monitors (model #110GS) viewed through cross-polarized filters (goggles) at a viewing distance of 100 cm. The dichoptic setting used two monitors placed at right angles with a beam splitter that combined the outputs of the two monitors. The left-eye and right-eye monitor outputs were passed through horizontal and vertical polarizing filters, respectively, before they reached a beam splitter. The observer viewed the display with passive polarizing glasses that ensured that each eye received the images presented on only one of the monitors (there was no crosstalk between the monitor signals, as measured with a Minolta CS-100 Chroma Meter). The screen had a resolution of 1024 × 768 pixels with a refresh rate of 85 Hz and a mean luminance at 46.2 cd/m^2. The gratings were contrast reversed at 6.07 Hz in the amblyopic/nondominant eye and at 8.5 Hz in the fellow/dominant eye of amblyopic/Control participants, as shown in Figure 1*A*. The contrast of the gratings in the amblyopic/nondominant eye (target contrast) was swept from 1.7 to 40% within a 10 s trial, and the mask contrast in the fellow/dominant eye was fixed at 20%. Specifically, the target contrast was swept over 10 logarithmic steps within 8.24 s duration, which included 10 sample epochs along with 2 additional epochs (one before and one after the sweep series) and yielded a 9.88 s trial with the frequency resolution at 1.21 Hz. Stimulus frequencies were chosen so that there were integer numbers of cycles in each epoch, and the harmonics of the two frequencies would be precisely represented in the spectrum. In this case, the frequencies 6.07 Hz and 8.5 Hz are five and seven times the resolution of 1.21 Hz, respectively. For demonstration purposes, in Figure 1*B*, the spectrum was from the experiment where the contrasts in both eyes were fixed and was calculated over an interval twice as long as the discrete level epochs in the sweep experiment, thus half the frequency step, with 0.607 Hz between adjacent frequencies. The associated Fourier spectrum from the SSVEP responses was dominated by self-terms at the second harmonic response to the target frequency (F: 2F1 at 12.14 Hz) and to the mask frequency (2F2 at 17 Hz), and also IM terms, which are the sum and difference of the monocular frequency inputs (F1 + F2 at 14.57 Hz, F1–F2 at 2.43 Hz), as shown in Figure 1*B*.

EEG data acquisition and source localization. We used 128-channel HydroCell Sensor Nets and the Net Station 300 acquisition system

Table 1. Clinical details of participants with amblyopia

Participant ID	Age	Gender	Diagnosis	Visual acuity (logMAR)		Stereoacuity	Deviation	Fusion	History
				Fellow eye	Amblyopic eye				
1	49	f	A	−0.2	0.498	800"	ortho	yes	patching done
2	21	m	A	−0.097	0.341	200"	ortho	yes	patching done
3	52	f	A	−0.04	0.518	200"	ortho	yes	patching done
4	48	f	A	0	0.301	70"	ortho	yes	patching done
5	50	m	A	0	0.7	800"	ortho	yes	patching done
6	50	f	A	0	0.739	200"	ortho	yes	patching done
7	26	f	A	−0.04	0.518	400"	ortho	yes	no patching
8	24	m	A	−0.02	0.224	70"	ortho	yes	no patching
9	32	f	A	−0.04	0.498	70"	ortho	yes	no patching
10	21	f	A	−0.097	0.301	100"	ortho	yes	patching done
11	27	m	S & A	−0.097	0.602	n/a	ET 16	yes	no patching
12	61	m	S & A	0	0.756	2000"	XT 4, R/L 20, DVD	yes	patching done
13	48	f	S & A	−0.097	0.498	n/a	XT 10	yes	surgery & patching
14	42	f	S & A	−0.077	0.224	n/a	L/R 15	yes	no patching
15	36	f	S & A	−0.097	0.538	n/a	ET 4	yes	surgery & patching
16	54	f	S	−0.077	0.224	1500"	ET 16, R/L 6	yes	surgery & patching
17	53	m	S	−0.04	0.341	n/a	ET 20, R/L 4	yes	no patching
18	34	f	S & A	0	0.377	n/a	XT 30, L/R12	yes	surgery & patching
19	67	f	S & A	−0.02	0.518	2000"	XT 8	yes	surgery & patching
20	34	f	S & A	0	0.518	n/a	XT 8	yes	surgery & patching
21	52	f	S & A	0	0.756	n/a	XT 20	No	no patching
22	53	f	S & A	−0.137	0.518	n/a	XT 2, L/R 17	No	surgery & patching
23	28	f	S & A	−0.097	0.498	n/a	XT 10, R/L12	No	no patching
24	65	f	S & A	0	0.301	n/a	ET 16, R/L 8	No	surgery & patching
25	29	m	S	−0.097	0.341	n/a	XT 12, R/L 4	No	patching done
26	58	m	S & A	−0.04	0.836	n/a	XT 14, L/R 14, DVD	No	surgery & patching
27	26	f	S & A	−0.097	0.224	n/a	XT 25	No	no patching

Deviation at near distance (33 cm) with the best optical correction is shown in prism diopters. A, Anisometropic amblyopia; S, strabismic amblyopia; S & A, mixed strabismus and anisometropia; DVD, Disassociated vertical deviation; XT, exotropia, ET, esotropia; L/R, left-eye hypertropia; R/L, right-eye hypertropia. n/a indicates that stereoacuity was not measurable with random dot Stereo Butterfly card.

(Magstim EGI) to collect EEG data from each participant with a bandpass filter from 0.1 to 50 Hz and digitized at 500 Hz. Each trial had a duration of ~10 s that was divided into 12 epochs (10 core + 1 prelude + 1 postlude), and with intervals of 3 ± 0.5 s (mean ± SD) between each trial. The prelude and postlude epochs were discarded for data analysis to eliminate stimulus onset/offset transients. A total of 20 trials was acquired from each participant at the best optical correction, and 5 min breaks were taken after every five trials. Participants were required to align the nonius line in each eye and instructed to fixate on a central marker and avoid blinking during stimulus presentation. The dichoptic setting itself allowed ~10° of adjustment of the visual angle horizontally to align the nonius lines. For Strab participants who had fusion, prisms were used if their eye deviation was beyond 10° horizontally and/or if they had vertical deviation. For the Strab participants who had no fusion, the prisms were used to adjust the nonius lines to the point that fusion was broken. After the EEG recording, three fiducials (nasion, right and left preauricular) and the 3D locations of 128 sensors were recorded for each participant at the end of the EEG session, using a FASTRAK radio frequency 3D digitizer (Polhemus). These 3D sensor location data were used to coregister to participants' T1-weighted anatomic magnetic resonance (MR) scans, in which a three-shell boundary element model of the skull and scalp was computed. A custom software package with postprocessed EEG signals and artifact rejection (eye movements and blinks) designed by the Norcia research group (Ales et al., 2013) was used for off-line EEG data processing and analysis.

The details of EEG source localization used in this study have been described previously (Appelbaum et al., 2006; Cottereau et al., 2011; Hou et al., 2016, 2017, 2020). In brief, each of the participants had structural and fMRI scans in a separate session to define cortical areas. MRI data were acquired on a 3T Siemens Prisma Fit scanner. Structural MRI scans covered the whole head at 0.8 mm^3 cubic voxel resolution and segmented using FreeSurfer (Martinos Center for Biomedical Imaging; https://surfer.nmr.mgh.harvard.edu/fswiki/FreeSurferMethodsCitation). Functional MRI had a resolution of 1.6 mm^3 cubic voxels with a repetition time of 1.5 s. Functional MRI data were corrected for motion artifacts using the FSL software library (FMRIB, Oxford, UK). The regions of interest (ROIs) corresponding to visual areas V1, V2v, V2d, V3v, V3d, V3a, and hV4 were defined by a procedure based on retinotopic mapping using fMRI (Engel et al., 1997), with rotating wedge and expanding ring stimuli created with Vistadisp software (VISTA Lab). Area hMT+ was identified using low-contrast motion stimuli (Huk and Heeger, 2002). The lateral occipital cortex (LOC) was defined using an fMRI localizer scan with stimuli from Kourtzi and Kanwisher (2000). All fMRI stimuli were presented in a block design with a 24 s cycle and viewed through a mirror on an LCD display behind the bore, providing a 12.6 degree diameter field of view. ROIs were defined using the mrVista MATLAB toolbox (VISTA Lab). Cortical source models were created with the MNE software package (Gramfort et al., 2014). Figure 1*C* shows a sample MRI scan from one participant to define the ROIs (V1, V3a, hV4, hMT+, and LOC) in visual cortex that were used to localize the sources of EEG scalp potentials. An L2 minimum norm inverse with sources constrained to the location and orientation of the cortical surface (Hämäläinen et al., 1993) was computed for EEG source localization.

ROI-based analysis. Because V1 is the first neural locus where the visual inputs from the two eyes are combined, we specifically examined responses in V1. The responses in extra-striate cortex, including V3a, hV4, hMT+, and LOC were also examined. We excluded the areas V2 and V3 because of the potential for cross-talk from other areas (Cottereau et al., 2011). The raw EEG recordings for each trial were divided into 10 sequential core epochs that corresponded to the swept contrast values so that we could measure contrast response functions. A recursive least-squares adaptive filter (Tang and Norcia, 1995) was used for each epoch to generate a series of complex-valued spectral coefficients representing the amplitude and phase of harmonic responses (Hou et al., 2007, 2017). To take into account the different noise levels for each participant (Vialatte et al., 2010), we computed the signal-to-

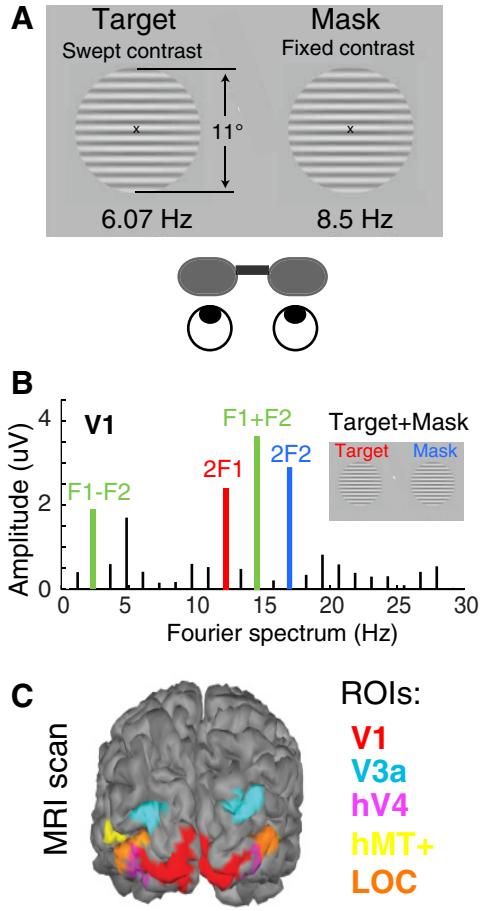

Figure 1. Illustration of stimuli and experimental design. ***A***, Dichoptic setting for a pair of parallel gratings that were contrast reversed with unique temporal frequency in each eye, viewed through cross-polarized goggles. The target contrast in the amblyopic/nondominant eye was swept from 1.7 to 40% in 10 logarithmic steps within a 10 s interval while the mask contrast in the fellow/dominant eye was fixed at 20%. ***B***, Fourier spectrum and dominant response components in V1 from one participant, with both target and mask contrasts set at 20%, for purposes of illustration. ***C***, Illustration of cortical ROIs defined by structural and fMRI from a sample participant.

noise ratio (SNR) for each participant by dividing peak amplitudes by the associated noise. The noise was defined for a given frequency by the average amplitude of the two neighboring frequencies (stimulus frequencies ± 1.21 Hz). The SNRs versus contrast response functions were obtained by coherently averaging the spectral coefficients for each epoch across trials for each participant, ROI, and harmonic component. Then, we averaged the SNRs incoherently across the participants in each group. There were no significant differences between left and right hemisphere for IM responses (F1 + F2 at 14.57 Hz) in V1 for both the Control ($p = 0.586$) and amblyopic ($p = 0.689$) groups when collapsing across ROIs; therefore, we averaged the data from both hemispheres for further analysis.

Contrast response modeling. The Tsai et al. (2012) model extended a well-established description of the contrast response function—the hyperbolic ratio function (Naka and Rushton, 1966; Albrecht and Hamilton, 1982)—and included a time varying contrast input that explained the full range of frequency-domain responses in a nondichoptic masking study. As described in Hou et al. (2020) and summarized below, we made several modifications to adapt the Tsai et al. (2012) model to fit data from our dichoptic masking paradigm in participants with normal binocular vision (Hou et al., 2020) as well as participants with disrupted binocular vision (the present study). The modifications from Tsai et al. (2012) include the following: (1) The target and mask stimuli were presented to different eyes, (2) a weighting factor for the target contrast input was used to model the relative contributions of the target and the mask contrast in our dichoptic masking study, and (3) an additive baseline parameter was used to account for the SNR floor not being ~1. Thus, the variant of the Tsai et al. (2012) model used in this study is described by the following:

$$c(x,t) = 2\sin[2\pi f_x x]\left\{w_{target}c_{target}\cos\left[2\pi f_{target}t\right] + c_{mask}\cos[2\pi f_{mask}t]\right\} \quad (1)$$

$$\hat{c}(t) = \left|\frac{c(x,t)}{2\sin[2\pi f_x x]}\right| = \left|w_{target}c_{target}\cos\left[2\pi f_{target}t\right] + c_{mask}\cos[2\pi f_{mask}t]\right| \quad (2)$$

$$u(t) = \frac{[\hat{c}(t)]^p}{[\hat{c}(t)]^q + [w_{target}\sigma]^q} \quad (3)$$

$$R(f) = R_0(f) + R_m|U(f)|. \quad (4)$$

Equation 1 defines the counterphase flicker of a sinusoidal grating over time and space $c(x,t)$, where c_{target} and c_{mask} are the contrasts of the Target and Mask, respectively, f_{target} and f_{mask} are the temporal frequencies (Bonin et al., 2006; Carandini, 2004; Tsai et al., 2012), and w_{target} is a weighting factor of target contrast relative to mask. Equation 2 is the absolute value of the contrast modulation at each point in space, normalized to its maximal value. Equation 3 defines the nonlinearity, where σ is a semisaturation constant representing contrast sensitivity, p is an exponent of the excitation, and q is an exponent of divisive suppression (Foley, 1994; Chen et al., 2001; Xing and Heeger, 2001; Peirce, 2007), as described in Tsai et al. (2012). Equation 4 is the function fit to the data, where $R(f)$ is the SNR at frequency f. The parameter R_0 is a frequency-dependent baseline parameter we added to account for the signal-to-noise floor, and R_m is the response gain factor. The notation $|U(f)|$ denotes the amplitude of the Fourier transform of time series $u(t)$ at frequency f. Parameter values were obtained by nonlinear constrained optimization (MATLAB function fmincon) to minimize the sum of the squared residual error. The coefficient of determination (R^2) was used to assess goodness of the model fits. The standard deviations and confidence intervals of the fit parameter values were estimated from the distributions of 1000 bootstrap resamplings, drawn randomly from participant data in each group with replacement.

Our model of binocular combination is linear up to the binocular summation stage, followed by divisive normalization and nonlinear exponents. This is different from the Meese et al. (2006) model and the Ding and Levi (2014) model for binocular combination, which have explicit stages of interocular suppression (normalization) before binocular combination. Our model is equivalent to these models if the nonlinear exponents at the monocular stages are set to 1, allowing a linear combination of the inputs from the two eyes. Thus, our version of the model does not differentiate whether the divisive normalization occurs before or after binocular combination.

Statistical analysis. Brown–Forsythe tests in MATLAB were used to test the homogeneity of variance for each factor (group, ROI) in Figures 2 and 4. The initial analyses were conducted in R using a mixed between- and within-subjects design ANOVA (Figs. 2, 4). The two-tailed heteroscedastic t tests were conducted in Microsoft Excel to identify the group differences in Figures 2 and 4, as well as visual acuity and age. Bonferroni correction was used to control the familywise error rate for repeated t tests in each group (Control, Aniso, and Strab) for Figure 2*B*, in which the significance level was 0.05/3 = 0.017. The group differences of the fit parameter values (Figs. 6, 7, 8) were identified by the Wilcoxon rank sum tests in MATLAB and Bonferroni corrected as well. The nested model F tests were conducted in MATLAB.

Results

Responses at IM frequency are significantly reduced along the visual cortical hierarchy in strabismic amblyopia

In SSVEP, the presence of IM terms tagged with combinations of the unique temporal frequencies presented to each eye is neural

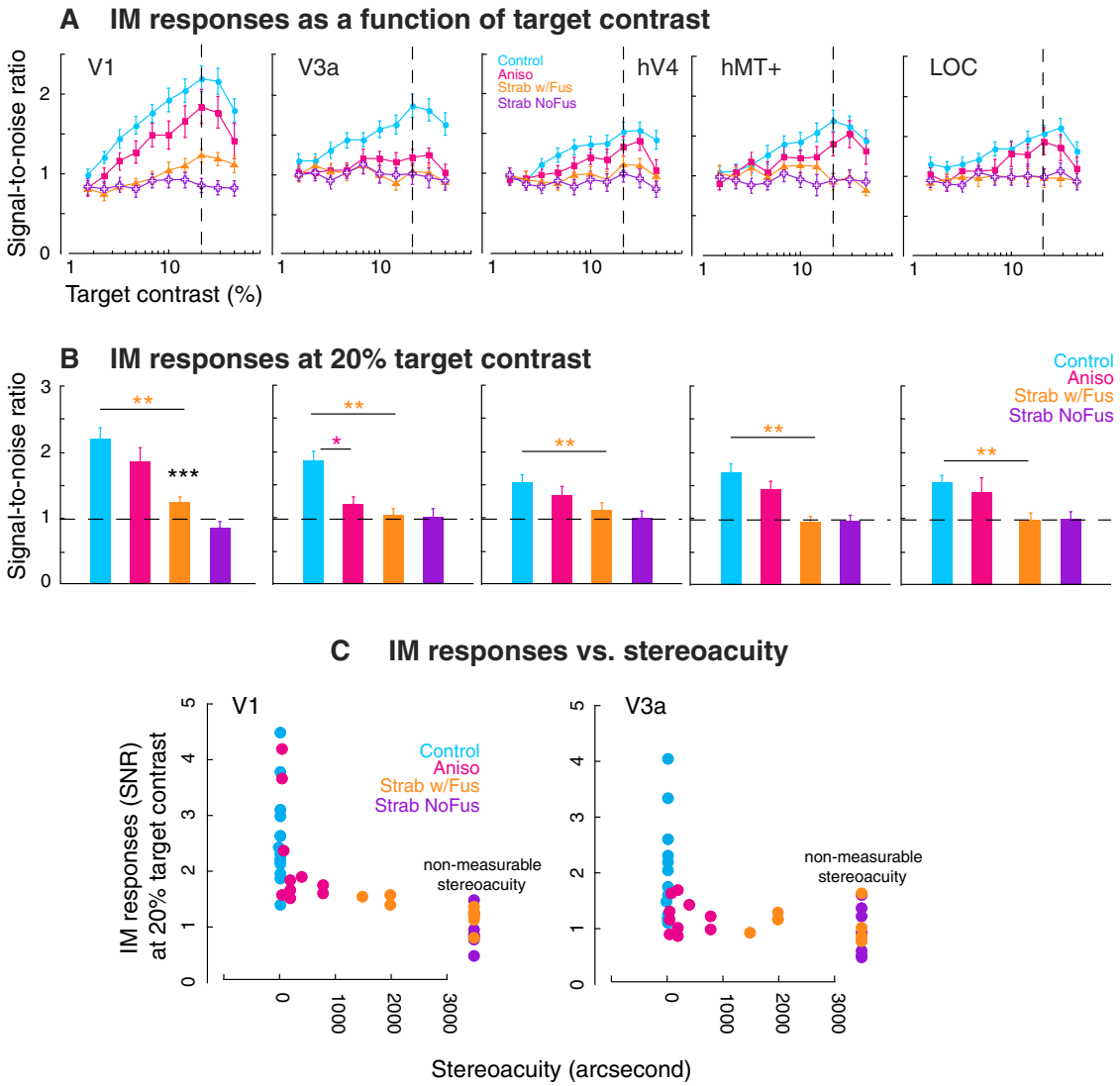

Figure 2. Profile of IM responses in the visual cortical hierarchy. Error bars indicate SEM. Colors denote groups as described in the legend. ***A***, Mean SNR of IM responses as a function of target contrast in four groups: Controls, Anisos, and Strabs with and without binocular fusion. Across all ROIs, the peak IM responses were near 20% target contrast (vertical dashed lines), where the target contrast matched mask contrast. ***B***, IM responses measured at 20% target contrast in four groups, where both the target and mask contrast were at 20%. Horizontal dashed lines indicate SNR floor of 1. Colored asterisks indicate statistical significance of group comparisons to Controls, and the black asterisk indicates *t* test against an SNR level of 1; significance levels $*p < 0.017$, $**p < 0.01$, and $***p < 0.001$. ***C***, IM responses (SNR) at 20% target contrast in V1 (left) and V3a (right) as a function of stereoacuity in individual participants. Fus, Fusion.

evidence for interocular interaction (Hou et al., 2020) as they can result only from the interaction of the inputs of the two eyes (Brown et al., 1999). Among the IM components, F1 + F2 at 14.57 Hz was dominant in our study as seen in Figure 1*B*; therefore, we used this particular IM component as an index of interocular interaction in the visual cortex.

Figure 2 plots the group mean of IM SNR as a function of target contrast in various cortical areas. As seen in Figure 2, when the target contrast in the amblyopic/nondominant eye was swept from 1.7 to 40%, and the mask contrast in the fellow/dominant eye was fixed at 20%, the IM responses across all ROIs in Controls (blue) was visible at low contrast (~2.5%) and continued to increase to a peak, where both target and mask contrasts were matched at 20% and then declined thereafter. Anisos showed a similar pattern to that of Controls, except for V3a, although overall response amplitudes seemed weaker than those in Controls. Strabs, including those with and without fusion (orange and purple, respectively), had diminished IM responses in all ROIs, except for V1 at high-target contrast (above 20%) in the subgroup with fusion. The homogeneity of variances for each of the two factors (group, $p > 0.05$; ROI, $p > 0.05$) was tested and revealed equal variances. An initial between-subject ANOVA with two factors (Group: Control, Aniso, and Strab; ROI: V1, V3a, hV4, and hMT+ and LOC) revealed significance ($F_{(1,39)} = 388.48$, $p < 0.001$). To reduce data dimensionality, we combined the Strab subgroups (with and without fusion) into one group and only picked the peak IM responses at 20% target contrast for the initial analysis. The interaction of ROI and group was not significant ($F_{(8,72)} = 1.50$, $p = 0.174$), suggesting that there was no significant difference in groups across ROIs. However, ROIs ($F_{(4,36)} = 3.19$, $p = 0.024$) and groups ($F_{(2,39)} = 12.18$, $p < 0.001$) were significant. The ROI differences were likely driven by the higher responses in V1 than in extra-striate cortex. This phenomenon has been observed in individuals with normal binocular vision (Hou et al., 2020). We further compared Anisos and Strabs near the peak IM responses (at 20% target contrast level) to Controls with two-tailed heteroscedastic *t* tests. Strabs-with-fusion had significantly lower SNRs than Controls across all

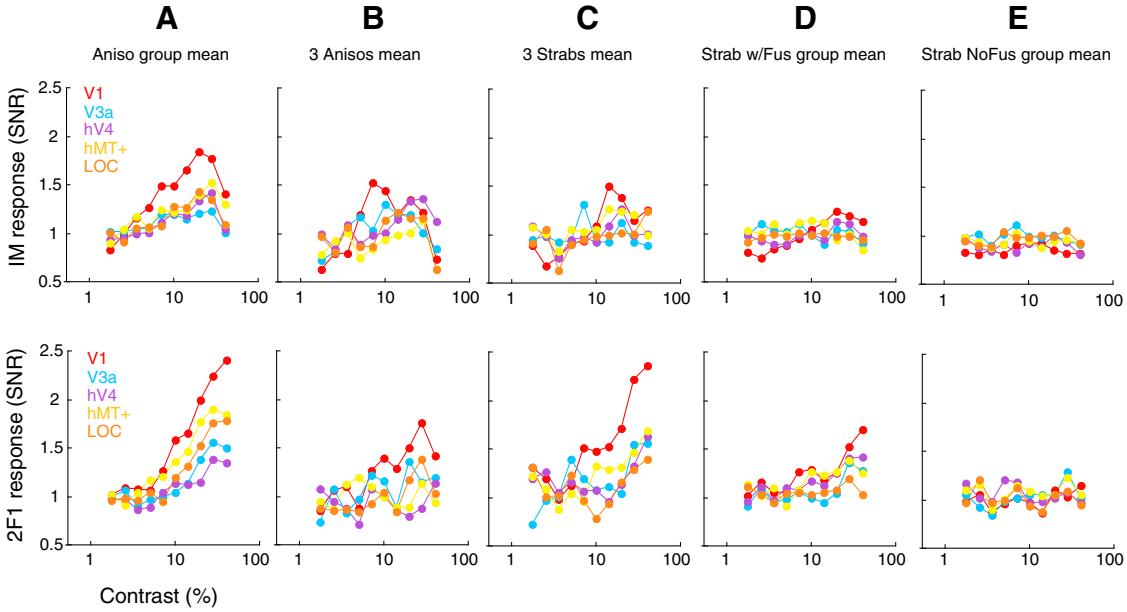

Figure 3. Mean SNR of IM (top row) and self-term (2F1, bottom row) responses as a function of target contrast in various visual areas. The Aniso group (***A***), three Anisos with poor stereoacuity (400″—800″) (***B***), three Strabs with measurable stereoacuity (1500″—2000″) (***C***), the Strab-with-fusion group (***D***) and the Strab with no fusion group (***E***). Colors denote cortical areas. Data for ***A***, ***D***, and ***E*** are replotted from Figures 2*A* and 4*A*. Fus, Fusion.

ROIs ($p < 0.01$), whereas Anisos had significantly lower SNRs than Controls only at V3a ($p < 0.05$). To determine if the IM response is significantly above the SNR floor level in Strabs, we performed a one-sample t test against an SNR of 1 for the peak IM. Responses in the Strab-with-fusion subgroup were significant only at V1 ($p < 0.05$) but not for extra-striate areas, whereas responses for the no-fusion subgroup were not significant in any ROI. This finding indicates that there are latent interocular interactions in the visual cortex when contrast is increased in the amblyopic eye of strabismic amblyopes. However, it appears this happens only for the individuals with binocular fusion, although this latent binocular interaction is still significantly weaker than that in normal binocular vision.

To explore the link between the IM responses and binocularity, we plot IM responses in V1 and V3a as a function of stereoacuity for each participant in Figure 2*C*. This relation demonstrates that measurable stereoacuity is related to IM responses above the noise floor (SNR = 1). Most anisometropic amblyopes have residual binocular function (i.e., have residual stereopsis; Table 1) and show some level of interocular interaction in visual cortex (Fig. 2*C*, red), whereas strabismic amblyopes (orange and purple) with worse or nonmeasurable stereoacuity had IM responses near the noise floor. This finding of reduced or absent interocular interaction is consistent with a previous psychophysical report of absence in binocular summation in strabismic amblyopia (Levi et al., 1979). Furthermore, we also compared IM responses for three Strabs who had measurable stereoacuity (1500″–2000″) to three Anisos who had poor stereoacuity (400″–800″), as well as to the full group mean of Anisos and Strabs, as seen in Figure 3 (top row). The IM responses of the three Strabs with measurable stereopsis (Fig. 3*C*) are similar to those of the three Anisos with the poorest stereopsis (Fig. 3*B*). In particular, there is a tendency for the IM term to decrease with decreasing binocularity (Fig. 3*A*–*E*), with a transition from a clear and strong peak IM response to nonexistent IM responses in V1 (red).

Responses at self-term frequencies are significantly reduced along the visual cortical hierarchy in strabismic amblyopia

The use of dichoptic parallel grating stimuli in each eye modulated at distinct temporal frequencies allowed us to quantify spectral components associated with the individual stimuli from monocular inputs (responses at self-term frequencies).

Target responses from the amblyopic eye (2F1)

Figure 4*A* plots the mean SNR of the target responses (2F1) from the amblyopic eye as a function of target contrast in various cortical areas, whereas the mask contrast was fixed at 20% in the fellow eye. As seen in Figure 4*A*, when target contrast was swept from 1.7 to 40%, the responses to the target across all ROIs were evident at ~7 to 10% target contrast and then increased monotonically until it saturated at ~ 28% target contrast in the Control (blue) group. The Aniso group (red) showed a similar pattern to that of the Control group but had weaker responses, especially for V3a. The Strab group with fusion (orange) did not show target responses in any ROI until the target contrast reached 20% and matched the mask contrast level. The Strab group without fusion (purple) barely showed target responses even at a high target contrast level (28%) in areas V3a and hMT+. Equal variances were revealed for each factor (group, $p > 0.05$; ROI, $p = 0.05$, after removing one outlier in Controls, $p > 0.05$). An initial between-subject ANOVA with two factors [Group: Control, Aniso, and Strab (combined subgroups); ROI: V1, V3a, hV4, and hMT+ and LOC] revealed significance ($F_{(1,39)} = 113.55$, $p < 0.001$). To reduce data dimensionality, we picked the peak response at 28% target contrast for the initial analysis. The interaction of ROI and group was significant ($F_{(8,72)} = 1.19$, $p = 0.049$), suggesting that there is a significant difference in groups at various ROIs. Then, we further compared Aniso and Strab groups at the peak responses to the Control group. The differences between Anisos and Controls did not reach significance in any of the five ROIs after Bonferroni correction. For the combined Strab group, SNR was significantly weaker than that of the Control group in V1 ($p < 0.01$), V3a ($p < 0.01$), and LOC ($p <$

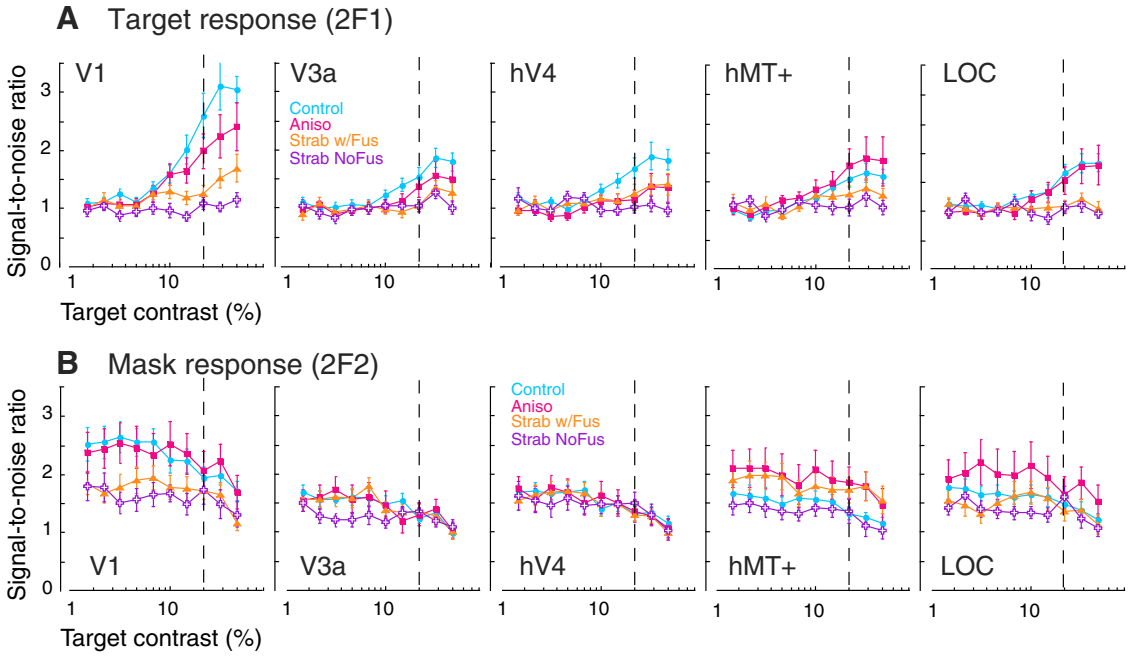

Figure 4. Mean SNR of self-term responses as a function of target contrast in different visual areas in four groups. Error bars indicate SEM. Colors denote groups. Vertical dashed lines indicate matched target and mask contrasts at 20%. ***A***, SNR to target stimuli that were swept from 1.7 to 40% of contrast in the amblyopic/nondominant eye. ***B***, SNR to mask stimuli that were fixed at 20% of contrast in the fellow/dominant eye. Fus, Fusion.

0.001) after Bonferroni correction, but the differences did not reach significance in hV4 and hMT+ after Bonferroni correction.

Furthermore, we also compared target responses from the amblyopic eye (2F1) for three Strabs who had measurable stereoacuity (1500″–2000″) to three Anisos who had poor stereoacuity (400″–800″), as well as to the full group mean of Anisos and Strabs, as seen in Figure 3 (bottom row). There is a tendency for the 2F1 responses to decrease with decreasing binocularity (Fig. 3*A*–*E*), with a transition from a clear and strong response to weak or nonexistent responses in V1 (red).

Mask responses from the fellow eye (2F2)

Figure 4*B* plots the mean SNR of the mask responses from the fellow/dominant eye at 20% fixed contrast as a function of target contrast in various cortical areas, whereas the target contrast was swept from 1.7 to 40% in the amblyopic/nondominant eye. As seen in Figure 4*B*, the responses to the mask (2F2) across all ROIs and all groups showed a similar masking trend as the target contrast increased; the responses to the mask frequency were high when target contrast was low (e.g., at 1.7%), and the responses decreased as the target contrast was increased to 40%. Equal variances were revealed for each factor (group, $p > 0.8$; ROI, $p > 0.8$). An initial between-subject ANOVA with two factors (target contrast level: 1.7% and 40%; ROI: V1, V3a, hV4, and hMT+ and LOC) revealed significance ($F_{(1,39)} = 149.98$, $p < 0.001$). There were significant differences among the ROIs ($F_{(4,36)} = 4.47$, $p = 0.005$) and target contrast level ($F_{(1,39)} = 37.24$, $p < 0.001$), indicating a masking effect from the amblyopic/nondominant eye to the fellow/dominant eye in various ROIs of four groups. However, there were no significant differences among groups ($F_{(2,39)} = 0.36$, $p = 0.702$). To reveal whether the masking effect has a similar trend across all groups, we further calculated the masking percentage defined as (2F2 at 1.7% − 2F2 at 40%)/(2F2 at 1.7%) across ROIs in four groups. A one-way between-subject ANOVA revealed no significant differences among groups ($F_{(2,39)} = 0.05$, $p = 0.956$) and ROIs ($F_{(4,36)} = 1.91$, $p = 0.130$), suggesting that the masking effect from the amblyopic eye to the fellow eye in both Anisos and Strabs was the same as the masking effect from the nondominant eye to the dominant eye in Controls across V1 and extra-striate cortex. As our paradigm used a mask of fixed contrast in the dominant/fellow eye, and as we did not include a mask-alone condition, we cannot directly compare the masking effect of each eye on the other.

A dichoptic gain control model fits both self- and IM-term responses

We modified a gain control model (Tsai et al., 2012), which can simultaneously fit both self- and IM-term responses in a target + mask paradigm to account for dichoptic masking in our study. This variant of the Tsai et al. (2012) model included the excitation (p) and divisive suppression (q) components, which provided critical information regarding the excitatory and suppressive contributions to binocular contrast interactions at each level of the visual cortical hierarchy. The model fits are shown in Figure 5, where the black solid lines indicate the best fitting model. The corresponding fit parameters and values in each ROI are listed on the right for each group. Several critical observations from our model fits are described below.

Excitatory and suppressive contributions to binocular contrast interactions

Our model fits revealed a different pattern of relationship between excitatory (p) and suppressive (q) contributions in binocular contrast interactions among Controls, Anisos, and Strabs-with-fusion. We excluded the Strabs-without-fusion subgroup because this group produced responses that were too weak to model. The excitatory (p) contribution to binocular contrast interactions in Strabs was significantly smaller than those in Controls and Anisos (Fig. 6*A*), whereas the suppressive (q) contribution was similar among the three groups (Fig. 6*B*). This is also further evident in Figure 6*C*, where the differences between the suppressive (q) and excitatory (p) exponents were

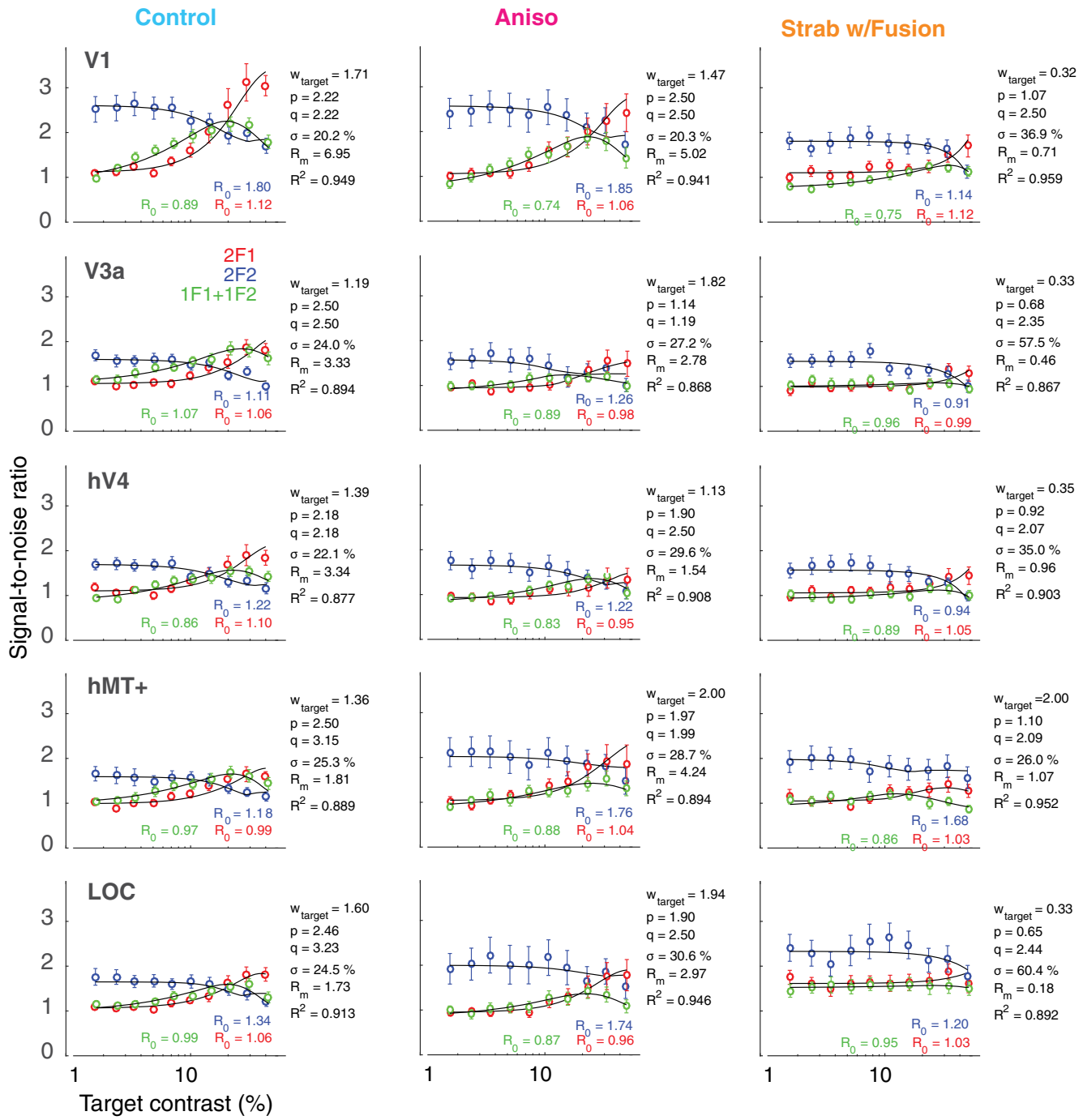

Figure 5. Fits of a variant of the Tsai et al. (2012) model to self-term and IM-term responses in different visual areas in three groups, Controls, Anisos, and Strabs-with-fusion. Data are replotted from Figures 2*A* and 4*A*,*B*. Target responses at 2F1 from the amblyopic/nondominant eye are shown in red; mask responses at 2F2 from the fellow/dominant eye are shown in blue, and the IM responses at F1 + F2 representing interocular interactions from the two eyes are shown in green. Error bars indicate SEM. Black solid lines indicate the best fitting model. The corresponding fit parameters in each ROI are listed on the right for each group. The fit parameters are semisaturation value (σ), excitatory (p) and suppressive (q) factors, response gain (R_m), weight of the amblyopic eye relative to the fellow eye (W_{target}), and goodness of fit (R^2). R_0 indicates a baseline parameter for each response component.

significantly larger in Strabs (orange) across all ROIs, compared with those in Anisos and Controls. This finding indicates greatly reduced excitation in visual cortex of strabismic amblyopia, whereas suppressive interactions remain intact.

Weaker contribution to binocular interactions from the amblyopic eye of strabismic amblyopes

We observed that the relative weight of the target contrast was on average 1.45 ± 0.21 SD across ROIs, compared with a weight of 1 in the mask eye in the Control group. The unequal weights between the eyes for Controls are likely because of our stimulus setting, in which the target eye had swept contrast, and the mask eye had a fixed contrast for a 8.24 s presentation that might have resulted in adaptation in the mask eye (Carandini et al., 1998; Dragoi et al., 2000). The Aniso group had a similar target weight (1.67 ± 0.37 SD) to that of the Control group. However, the Strab-with-fusion group had an average contrast weight of 0.33 ± 0.12 SD across all ROIs except for area hMT+ (W_{target} =

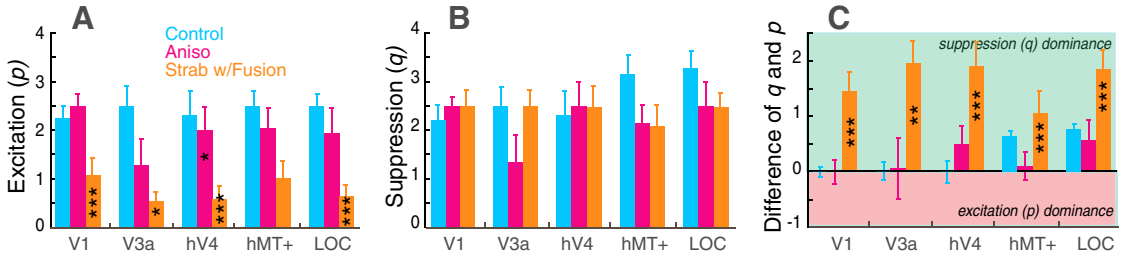

Figure 6. Estimated values of excitation (p) and suppression (q) from Figure 5 across ROIs in the three groups. Colors denote groups. Error bars indicate SD, estimated from bootstrap samples. ***A***, Across ROIs, excitatory (p) values were on average 2.4, 1.9, and 0.8 in the Control, Aniso, and Strab groups, respectively. ***B***, Across ROIs, suppressive (q) values were on average of 2.7, 2.2, and 2.4 in Strab, Aniso, and Control groups, respectively. ***C***, The differences between suppressive (q) and excitatory (p) exponents were significantly larger in the Strab group (orange) across all ROIs, compared with those in the Aniso and Control groups. The areas highlighted in green and pink indicate suppression (q) and excitatory (p) dominance, respectively; significance levels $^{*}p < 0.017$, $^{**}p < 0.01$, and $^{***}p < 0.001$, respectively.

2; Fig. 7*A*, orange), which is at least four times smaller than the value of Controls. This finding indicated that in strabismic amblyopes, the contribution of the amblyopic eye (target contrast) to binocular contrast interactions was attenuated. This suggests that binocular contrast interactions in the visual cortex are dominated by the visual input from the fellow eye in strabismic amblyopia and are extremely imbalanced compared with normal binocular vision.

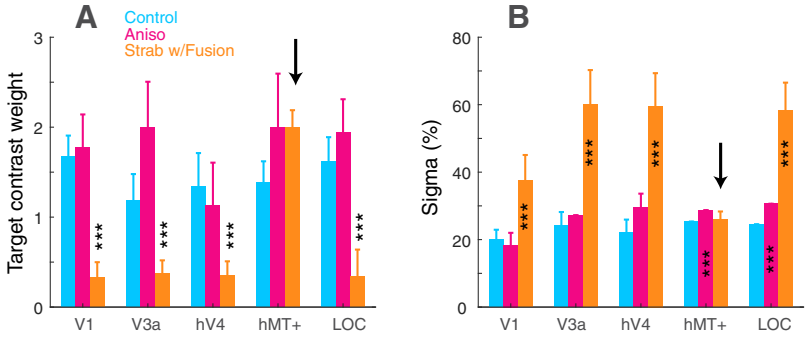

Figure 7. Estimated values of target contrast weight and semisaturation constant. Target contrast weight (***A***) and semisaturation constant, σ (***B***) estimated from the fits in Figure 5 across ROIs in three groups. Colors denote groups. Error bars indicate SD from the bootstrap samples. ***A***, The relative values of target weight (W_{target}) in the amblyopic eye across all ROIs, except for hMT+, were greatly increased in the Strab group compared with the values in the Control and Aniso group. ***B***, The values of σ across all ROIs, except for hMT+ in Strab group, were also increased, compared with the values in Control and Aniso groups. $^{***}p < 0.001$ significance level.

Rightward shifts of contrast response function in amblyopia

Our model fits showed a rightward shift of the contrast response function in amblyopic participants, particularly in strabismic amblyopes, compared with that in normal-vision observers. This is evident in Figure 7*B*, in which the values of the semisaturation constant (σ) across all ROIs, except for hMT+, were substantially increased in the Strab group. The Aniso group had slightly increased σ in areas hMT+ and LOC, compared with the values in the Control group.

In our variant of the Tsai et al. (2012) model, we have added parameters (e.g., R_0 and W_{target}) to fit our dichoptic study. The parameter R_0 was an additive baseline parameter that was used to account for the SNR floor not being ~1. The parameter W_{target} was the relative contributions of the target and the mask contrast in our dichoptic study. To determine the contributions of these added parameters, we conducted nested model F tests for the full model versus reduced versions of the model where one parameter at a time was set at a fixed value. The reduced model variants include the following: $R_0 = 1$, $W_{target} = 1$, as well as $p = q$ for each of the three groups (Controls, Anisos, and Strabs-with-fusion) in both V1 and extra striate cortex (hV4). The tests revealed that the baseline parameter R_0 was significant in both V1 and hV4 for all three groups ($p < 0.01$). W_{target} was a significant fit parameter for all three groups in V1 ($p < 0.001$) but was only significant for the Strab-with-fusion group in hV4 ($p < 0.001$). Recall that the W_{target} parameter in our study captures two contributions to the differential weighing of each eye's input, (1) the attenuation of the input in the weaker eye (equivalent to the attenuation proposed by Baker et al. (2008) and (2) the differential effectiveness of the swept contrast stimulus in the nondominant eye versus the fixed contrast stimulus in the dominant eye. In our previous work on data from normal-vision observers (Hou et al., 2020), we proposed that the relative lower weight of the fixed contrast input might be because of adaptation during the 8.24 s grating stimulus presentation. Previous electrophysiological studies have shown a strong orientation-selective adaptation in macaque V1 after prolonged exposure (>10 s; Carandini et al., 1998; Dragoi et al., 2000). It is possible that these adaptation effects are less pronounced in hV4 for Controls and Anisos, leading to nonsignificant effects of keeping the W_{target} parameter fixed. However, W_{target} has a significant effect for the Strab-with-fusion group, both in V1 and in extra-striate cortex ($p < 0.01$), consistent with previous studies (Baker et al., 2008; Chadnova et al., 2017). Setting $p = q$ had a significant effect in both V1 ($p = 0.01$) and hV4 ($p = 0.001$) for the Strab-with-fusion group but not for the Control and Aniso groups ($p > 0.1$). These findings suggest that in addition to the attenuation of visual input from the weaker eye of strabismic amblyopes, the relative strength of excitatory and suppressive interactions is altered when binocularity is disrupted.

Response gain reduced at V1 in amblyopia

We have seen that the response strength in general was weaker in amblyopia including both the Aniso and Strab groups, compared with the strength in the Control group (Figs. 2*A*, 4*A*). These were also characterized primarily by changes to the response gain factor (R_m), which are evident in Figure 8. Previous studies have shown that the response gain in V1 was about a factor of 2 higher than in extra-striate cortex in normal binocular vision (Hagler, 2014; Hou et al., 2020). We

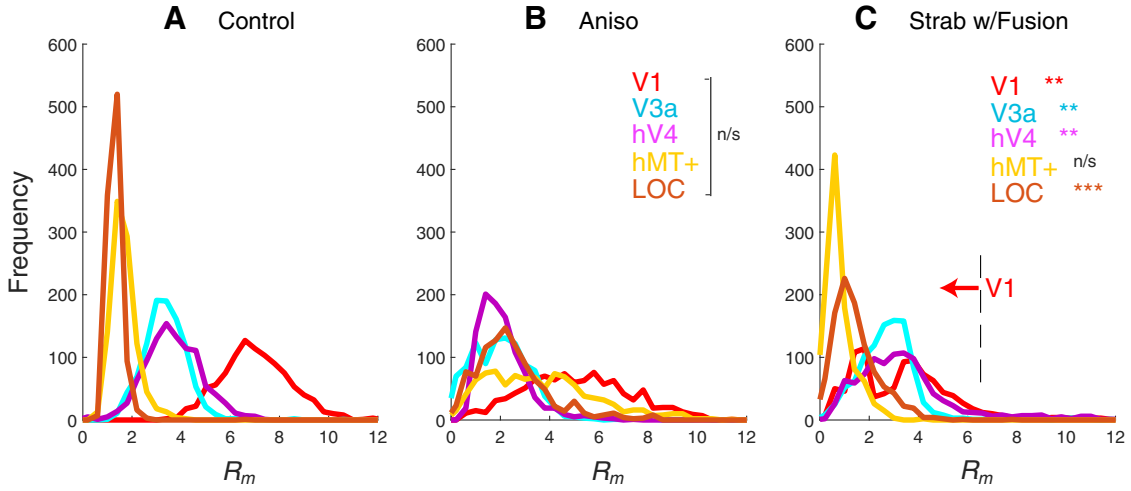

Figure 8. Histograms of response gain (R_m) from the bootstrap samples across ROIs in ***A***, Control, ***B***, Asino, and ***C***, Strab groups. Colors denote the ROIs. The response gain (R_m) in Strabs was lower across all ROIs, except for hMT+, compared with the Control group. R_m was a factor of 2 higher in V1 than in extrastriate cortex in both Control and Aniso groups. The vertical dashed line marks the mean response gain in V1 for the Control group; significance levels $^{**}p < 0.01$ and $^{***}p < 0.001$, respectively.

observed a similar phenomenon in the Control (Fig. 8*A*) and Aniso (Fig. 8*B*) groups in our study, although the Aniso group had slightly weaker response strength in V1 with a broader distribution of bootstrapped values compared with the Control group. However, no significant differences were found between the Control and Aniso groups across all ROIs. Strabs had substantially reduced strength in V1 compared with the Control group, as seen in the histograms in Figure 8*C*. Except for area hMT+, all ROIs had significantly weaker response gain in Strabs than in Controls.

Our model fits show that the low response strength of the Strab group is consistent with a reduced excitation p across all ROIs (Fig. 6*A*), as well as low response gain R_m (Fig. 8*C*), compared with the Control group. To determine if the weak responses in the Strab group are better characterized by a low response gain (R_m), or by low excitatory (p) exponent, we refit the model keeping one of these terms fixed while allowing the other terms to vary. Both variants yielded good fits to the data with the value of R_m, inversely related to the value of p. However, the main characteristic of the fits (whether p or R_m was fixed) was that the suppressive exponent (q) had to be greater than the excitatory exponent (p) to obtain a good fit of the model, further indicating that excitation was truly weaker in strabismic amblyopia. Model variants that constrained the ratio q/p to 1 generally provided worse fits to the data.

Discussion

In the present study, we investigated neural dynamics of normal and disrupted binocular contrast interactions along the visual cortical hierarchy, including V1 and extra-striate cortical areas V3a, hV4, HMT+, and LOC, using source-imaged SSVEP and frequency-domain analysis of dichoptic stimuli over a wide range of relative contrast between the two eyes. We found there are two forms of binocular interactions in the visual cortex that are disrupted severely in strabismic amblyopia but not in anisometropic amblyopia. One form is a direct measure of interocular interaction represented by IM terms between inputs from the two eyes, which was found greatly disrupted in the visual cortical hierarchy of strabismic amblyopes (Fig. 2). This finding is consistent with a previous VEP study using a similar approach on strabismic monkeys (Baitch et al., 1991) and a behavioral study that reported an absence of binocular summation in human strabismus and amblyopia (Levi et al., 1979). Another form is self-term responses to individual stimuli, which were also found to be greatly reduced in the visual cortex of strabismic amblyopes. This finding is consistent with an MEG study of V1 in human strabismic amblyopes (Chadnova et al., 2017). Importantly, the current study further quantified the magnitude of these effects with a gain-control model that includes a more complete profile of excitatory and suppressive contributions in binocular interactions. Similar to our previous results in participants with normal binocular vision (Hou et al., 2020), we were able to document these interactions along the human visual cortical hierarchy, including V1 and extra-striate cortex in disrupted binocular vision, such as strabismic amblyopia.

Excitatory contributions to binocular interactions are reduced in strabismic amblyopia, whereas suppression contributions are intact

Our model fits revealed different patterns of binocular interaction along the visual cortical hierarchy in normal and disrupted binocular vision, particularly in terms of excitatory and suppressive contributions. Our fit results showed greatly reduced excitation (p) in both V1 and extra-striate areas V3a, hV4, and LOC, except for hMT+, in human strabismic amblyopia (Fig. 6*A*), whereas suppressive interactions (q) remained intact with no change compared with normal vision observers (Fig. 6*B*). This finding suggests that although strabismic amblyopia disrupted the normal excitatory interactions between the two eyes, cortical inhibitory binocular connections were not disrupted, which leads to a dominance of suppressive interactions in striate and extra-striate (Fig. 6*C*). This finding is in agreement with physiological reports of V1 and V2 in amblyopic macaque monkeys (Hallum et al., 2017), which found that excitatory drive from the fellow eye dominated amblyopic visual cortex, especially in more severe amblyopes, but that suppression from both the amblyopic eye and the fellow eye was prevalent in all amblyopic animals. Our results provide robust electrophysiological evidence supporting the proposal that disruption of binocularity in strabismus or amblyopia is because of preferential loss of excitatory intrinsic connections between neighboring ocular dominance columns, leaving only inhibitory projections in the majority of neurons

(Sengpiel & Blakemore, 1996). Furthermore, our study provides a more complete profile regarding how excitatory and suppressive interactions contribute to the disruption of binocularity in humans not only in V1 but also in various extra-striate visual cortices.

Imbalanced contribution to binocular contrast interactions between the eyes in strabismic amblyopia

One of the critical parameters in our model fits is contrast weight in the amblyopic eye (W_{target}), which determines the relative contribution of the two eyes in binocular contrast interactions (the mask contrast had a fixed weight of one). Our model fits revealed that the relative contribution of the amblyopic eye (target contrast) to binocular contrast interactions in strabismic amblyopes was about a factor of three weaker than that of the fellow eye (mask contrast) across all ROIs, except for area hMT, which showed a similar weight to that of the Control group (Fig. 7*A*). However, the relative contribution of the amblyopic eye to binocular contrast interactions in anisometropic amblyopia was similar to the nondominant eye of the Control group. This indicated that the visual inputs from the two eyes were extremely imbalanced in strabismic amblyopes but not in anisometropic amblyopes, compared with normal binocular vision. This finding is consistent, at least in part, with a previous study that measured responses of single units in V1 of strabismic monkeys to dichoptic stimuli and attributed the observed binocular deficits to a reduction in functional inputs from one eye rather than an aberrant form of binocular interaction (Smith et al., 1997). A previous source-imaged MEG study (Chadnova et al., 2017) also reports a similar effect in human strabismic amblyopes. Chadnova et al. (2017) reported that the average attenuation in the amblyopic eye in V1 was ~0.21 relative to the fellow eye, indicating that the amblyopic eye is five times weaker than the fellow eye. One of the reasons our data showed less disruption of binocular interactions (amblyopic eye is only three times weaker) might be because we only include strabismic amblyopes with fusion in the model fits. Overall, our results with low W_{target} values in strabismic amblyopes along with the findings from single-neuron recordings and MEG/EEG measurements are in agreement with the proposal of attenuation of the visual input from the amblyopic eye in a psychophysical study (Baker et al., 2008). However, our study differs from these studies (Smith et al.,1997; Baker et al., 2008; Chadnova et al., 2017), as it reveals not only weak input from the amblyopic eye of strabismic amblyopes (low W_{target}), but also poor excitation (low p term), resulting in poor binocular interactions.

Selectivity in disruption of binocularity in extra-striate cortex

Our model fits revealed selective disruption of binocularity in the extra-striate cortex particularly in strabismic amblyopia. For example, although other extra-striate areas showed greatly increased imbalance to binocular interactions between the eyes (W_{target}~0.33; Fig. 6*A*) and σ (Fig. 7*B*), as well as excitation (p; Fig. 6*A*), area hMT+ showed normal values of these parameters in strabismic amblyopes as compared with the Control group. The difference between excitation (p) and suppression (q) in hMT+ was also smaller than in other extra-striate areas (Fig. 6*C*). It is not clear why hMT+ is relatively spared from disruption of binocular contrast interaction, as previous studies have not specifically investigated binocularity in extra-striate cortex.

Another example of selective disruption of binocularity in the extra-striate cortex is that interocular interactions (IM responses) in the Aniso group were significantly reduced in V3a compared with those of the Control group (Fig. 2*B*), and responses in other extra-striate areas (i.e., hV4, hMT+ and LOC) were similar in these two groups. The Strab group had diminished IM responses in all extra-striate areas; therefore, the selective disruption of binocularity in the extra-striate areas is less clear. This finding points to the important role of V3a in processing binocular vision and disparity information in monkeys (Hubel et al., 2015; Tsao et al., 2003) and humans (Cottereau et al., 2011). Compared with other areas in extra-striate cortex, our results indicate that V3a is more vulnerable to disrupted binocularity, which is consistent with its role as an important cortical area for binocular vision.

Latent binocular interactions in amblyopic visual cortex

Our study revealed there are latent interocular interactions in the visual cortex when stimulus contrast is increased to the amblyopic eye in strabismic amblyopes. We found that although strabismic amblyopia had greatly reduced interocular interactions represented by the IM responses, individuals with residual binocular fusion, but not individuals without fusion, showed a weak IM response in V1 at high contrast in the amblyopic eye (Fig. 2*A*, left). This is consistent with a behavioral study in human strabismic amblyopia, which reported the presence of binocular summation when the contrast in the amblyopic eye was adjusted to equate monocular sensitivities (Baker et al., 2007). Our results provided electrophysiological evidence of latent interocular interactions in early visual cortex in strabismic amblyopes who have residual binocular functions, such as fusion. In contrast, anisometropic amblyopes had a pattern of interocular interaction (IM responses) that was only slightly weaker than the pattern for individuals with normal binocular vision. This is likely because individuals with anisometropic amblyopia had residual binocular function, such as reduced but measurable stereoacuity, whereas the majority of strabismic amblyopes had severely disrupted binocular function and had no measurable stereoacuity (Table 1). Thus, our results are consistent with the McKee et al. (2003) study, which suggests that binocularity is a good index of visual contribution of the amblyopic eye.

In conclusion, our model fits revealed different patterns of binocular interaction between normal and amblyopic vision. In addition to attenuation of visual input from the nonfixating weaker eye, strabismic amblyopia had significantly reduced excitatory contributions to binocular interactions while leaving suppressive contributions intact. Our results provide robust evidence supporting the view that disruption of binocular interactions in strabismus or amblyopia is because of preferential loss of excitatory interactions between the eyes.

References

Albrecht DG, Hamilton DB (1982) Striate cortex of monkey and cat: contrast response function. J Neurophysiol 48:217–237.

Ales JM, Appelbaum LG, Cottereau BR, Norcia AM (2013) The time course of shape discrimination in the human brain. Neuroimage 67:77–88.

Appelbaum LG, Wade AR, Vildavski VY, Pettet MW, Norcia AM (2006) Cue-invariant networks for figure and background processing in human visual cortex. J Neurosci 26:11695–11708.

Baitch LW, Ridder WH, 3rd, Harwerth RS, Smith EL 3rd (1991) Binocular beat VEPs: losses of cortical binocularity in monkeys reared with abnormal visual experience. Invest Ophthalmol Vis Sci 32:3096–3103.

Baker DH, Meese TS, Mansouri B, Hess RF (2007) Binocular summation of contrast remains intact in strabismic amblyopia. Invest Ophthalmol Vis Sci 48:5332–5338.

Baker DH, Meese TS, Hess RF (2008) Contrast masking in strabismic amblyopia: attenuation, noise, interocular suppression and binocular summation. Vision Res 48:1625–1640.

Bonin V, Mante V, Carandini M (2006) The statistical computation underlying contrast gain control. J Neurosci 26:6346–6353.
Brown RJ, Candy TR, Norcia AM (1999) Development of rivalry and dichoptic masking in human infants. Invest Ophthalmol Vis Sci 40:3324–3333.
Campbell FW, Green DG (1965) Monocular versus binocular visual acuity. Nature 208:191–192.
Carandini M (2004) Receptive fields and suppressive fields in the early visual system. In: The Cognitive Neurosciences (Gazzaniga MS, Ed), pp 1–20. Cambridge, MA: MIT.
Carandini M, Movshon JA, Ferster D (1998) Pattern adaptation and cross-orientation interactions in the primary visual cortex. Neuropharmacology 37:501–511.
Chadnova E, Reynaud A, Clavagnier S, Hess RF (2017) Latent binocular function in amblyopia. Vision Res 140:73–80.
Chen CC, Kasamatsu T, Polat U, Norcia AM (2001) Contrast response characteristics of long-range lateral interactions in cat striate cortex. Neuroreport 12:655–661.
Cottereau BR, McKee SP, Ales JM, Norcia AM (2011) Disparity-tuned population responses from human visual cortex. J Neurosci 31:954–965.
Ding J, Levi DM (2014) Rebalancing binocular vision in amblyopia. Ophthalmic Physiol Opt 34:199–213.
Dorr M, Kwon M, Lesmes LA, Miller A, Kazlas M, Chan K, Hunter DG, Lu ZL, Bex PJ (2019) Binocular summation and suppression of contrast sensitivity in strabismus, fusion and amblyopia. Front Hum Neurosci 13:234.
Dragoi V, Sharma J, Sur M (2000) Adaptation-induced plasticity of orientation tuning in adult visual cortex. Neuron 28:287–298.
Engel SA, Glover GH, Wandell BA (1997) Retinotopic organization in human visual cortex and the spatial precision of functional MRI. Cereb Cortex 7:181–192.
Foley JM (1994) Human luminance pattern-vision mechanisms: masking experiments require a new model. J Opt Soc Am A Opt Image Sci Vis 11:1710–1719.
Gramfort A, Luessi M, Larson E, Engemann DA, Strohmeier D, Brodbeck C, Parkkonen L, Hamalainen MS (2014) MNE software for processing MEG and EEG data. Neuroimage 86:446–460.
Hämäläinen M, Hari R, Ilmoniemi RJ, Knuutila J, Lounasmaa OV (1993) Magnetoencephalography: theory, instrumentation and applications to noninvasive studies of the human brain. Rev Mod Phys 65:413–497.
Hagler DJ Jr (2014) Optimization of retinotopy constrained source estimation constrained by prior. Hum Brain Mapp 35:1815–1833
Hallum LE, Shooner C, Kumbhani RD, Kelly JG, Garcia-Marin V, Majaj NJ, Movshon JA, Kiorpes L (2017) Altered balance of receptive field excitation and suppression in visual cortex of amblyopic macaque monkeys. J Neurosci 37:8216–8226.
Harwerth RS, Smith EL, 3rd, Crawford ML, von Noorden GK (1984) Effects of enucleation of the nondeprived eye on stimulus deprivation amblyopia in monkeys. Invest Ophthalmol Vis Sci 25:10–18.
Hess RF, Thompson B, Baker DH (2014) Binocular vision in amblyopia: structure, suppression and plasticity. Ophthalmic Physiol Opt 34:146–162.
Holmes JM, Clarke MP (2006) Amblyopia. Lancet 367:1343–1351.
Hou C, Good WV, Norcia AM (2007) Validation study of VEP vernier acuity in normal-vision and amblyopic adults. Invest Ophthalmol Vis Sci 48:4070–4078.
Hou C, Kim YJ, Lai XJ, Verghese P (2016) Degraded attentional modulation of cortical neural populations in strabismic amblyopia. J Vis 16:16 1–16.
Hou C, Kim YJ, Verghese P (2017) Cortical sources of Vernier acuity in the human visual system: an EEG-source imaging study. J Vis 17(6):2 1–12.
Hou C, Nicholas SC, Verghese P (2020) Contrast normalization accounts for binocular interactions in human striate and extra-striate visual cortex. J Neurosci 40:2753–2763.
Huang CB, Zhou J, Lu ZL, Zhou Y (2011) Deficient binocular combination reveals mechanisms of anisometropic amblyopia: signal attenuation and interocular inhibition. J Vis 11(6):4 1–17.
Hubel DH, Wiesel TN (1965) Binocular interaction in striate cortex of kittens reared with artificial squint. J Neurophysiol 28:1041–1059.
Hubel DH, Wiesel TN, Yeagle EM, Lafer-Sousa R, Conway BR (2015) Binocular stereoscopy in visual areas V-2, V-3, and V-3A of the macaque monkey. Cereb Cortex 25:959–971.
Huk AC, Heeger DJ (2002) Pattern-motion responses in human visual cortex. Nat Neurosci 5:72–75.
Kourtzi Z, Kanwisher N (2000) Cortical regions involved in perceiving object shape. J Neurosci 20:3310–3318.
Lema SA, Blake R (1977) Binocular summation in normal and stereoblind humans. Vision Res 17:691–695.
Levi DM, Harwerth RS, Smith EL (1980) Binocular interactions in normal and anomalous binocular vision. Doc Ophthalmol 49:303–324.
Levi DM, Harwerth RS, Smith EL (1979) Humans deprived of normal binocular vision have binocular interactions tuned to size and orientation. Science 206:852–854.
Lowel S, Singer W (1992) Selection of intrinsic horizontal connections in the visual cortex by correlated neuronal activity. Science 255:209–212.
Mansouri B, Thompson B, Hess RF (2008) Measurement of suprathreshold binocular interactions in amblyopia. Vision Res 48:2775–2784.
McKee SP, Levi DM, Movshon JA (2003) The pattern of visual deficits in amblyopia. J Vis 3:380–405.
Meese TS, Georgeson MA, Baker DH (2006) Binocular contrast vision at and above threshold. J Vis 6:1224–1243.
Naka KI, Rushton WA (1966) S-potentials from luminosity units in the retina of fish (*Cyprinidae*). J Physiol 185:587–599.
Pardhan S, Gilchrist J (1992) Binocular contrast summation and inhibition in amblyopia. The influence of the interocular difference on binocular contrast sensitivity. Doc Ophthalmol 82:239–248.
Peirce JW (2007) The potential importance of saturating and supersaturating contrast response functions in visual cortex. J Vis 7(6):13 1–10.
Sengpiel F, Blakemore C (1996) The neural basis of suppression and amblyopia in strabismus. Eye (Lond) 10: 250–258.
Simons K (2005) Amblyopia characterization, treatment, and prophylaxis. Surv Ophthalmol 50:123–166.
Smith EL, Chino YM, Ni J, Cheng H, Crawford ML, Harwerth RS (1997) Residual binocular interactions in the striate cortex of monkeys reared with abnormal binocular vision. J Neurophysiol 78:1353–1362.
Tang Y, Norcia AM (1995) An adaptive filter for steady-state evoked responses. Electroencephalogr Clin Neurophysiol 96:268–277.
Tsai JJ, Wade AR, Norcia AM (2012) Dynamics of normalization underlying masking in human visual cortex. J Neurosci 32:2783–2789.
Tsao DY, Vanduffel W, Sasaki Y, Fize D, Knutsen TA, Mandeville JB, Wald LL, Dale AM, Rosen BR, Van Essen DC, Livingstone MS, Orban GA, Tootell RB (2003) Stereopsis activates V3A and caudal intraparietal areas in macaques and humans. Neuron 39:555–568.
Vialatte FB, Maurice M, Dauwels J, Cichocki A (2010) Steady-state visually evoked potentials: focus on essential paradigms and future perspectives. Prog Neurobiol 90:418–438.
Woodruff G, Hiscox F, Thompson JR, Smith LK (1994) The presentation of children with amblyopia. Eye (Lond) 8 (Pt 6): 623–626.
Xing J, Heeger DJ (2001) Measurement and modeling of center-surround suppression and enhancement. Vision Res 41:571–583.